THE JOURNAL OF BIOLOGICAL CHEMISTRY VOL. 288, NO. 2, pp. 1047–1054, January 11, 2013

Effect of Mutations of Arginine 94 on Proton Pumping, Electron Transfer, and Superoxide Anion Generation in Cytochrome *b* of the bc_1 Complex from *Rhodobacter sphaeroides*[*]

Received for publication, July 31, 2012, and in revised form, November 21, 2012 Published, JBC Papers in Press, December 3, 2012, DOI 10.1074/jbc.M112.397521

Yuan-Gang Qu[1], **Fei Zhou, Linda Yu, and Chang-An Yu**

From the Department of Biochemistry and Molecular Biology, Oklahoma State University, Stillwater, Oklahoma 74078

Background: The bc_1 complex catalyzes electron transfer from ubiquinol to cytochrome *c* and translocates protons across the membrane.
Results: Substitution of Arg-94 decreased the electron transfer activity and proton pumping capability and increased the superoxide production.
Conclusion: Arg-94 is an important amino acid for the proton pumping capability of the bc_1 complex.
Significance: The result is significant for understanding the catalytic mechanism of the bc_1 complex.

Proton transfer involving internal water molecules that provide hydrogen bonds and facilitate proton diffusion has been identified in some membrane proteins. Arg-94 in cytochrome *b* of the *Rhodobacter sphaeroides* bc_1 complex is fully conserved and is hydrogen-bonded to the heme propionate and a chain of water molecules. To further elucidate the role of Arg-94, we generated the mutations R94A, R94D, and R94N. The wild-type and mutant bc_1 complexes were purified and then characterized. The results show that substitution of Arg-94 decreased electron transfer activity and proton pumping capability and increased O_2^- production, suggesting the importance of Arg-94 in the catalytic mechanism of the bc_1 complex in *R. sphaeroides*. This also suggests that the transport of H^+, O_2, and O_2^- in the bc_1 complex may occur by the same pathway.

The cytochrome bc_1 complex (also known as ubiquinol-cytochrome *c* oxidoreductase or complex III) is a multisubunit dimeric integral membrane protein complex. It is an essential segment of cellular energy-conserving electron transport chains in animals, plants, and bacteria (1, 2). This complex catalyzes electron transfer from ubiquinol to cytochrome *c* (or cytochrome c_2 in bacteria) and concomitantly translocates protons across the membrane to generate a membrane potential and pH gradient for ATP synthesis. The cytochrome bc_1 complexes from all species contain three core subunits, cytochrome *b*, cytochrome c_1, and the Rieske iron-sulfur protein, which house two *b*-type cytochromes (b_H and b_L), one *c*-type cytochrome (c_1), and a high potential Rieske [2Fe-2S] cluster, respectively. Depending on the source, the cytochrome bc_1 complexes contain various numbers (zero to eight) of non-redox group-containing subunits, also called supernumerary subunits (3–5).

Intensive biochemical and biophysical studies on this complex (6–8) have led to the formulation of the "protonmotive Q-cycle" mechanism for electron and proton transfer in this complex (9–11). In the Q-cycle mechanism, it is postulated that the first electron of ubiquinol is transferred to the "high potential chain," consisting of the Rieske iron-sulfur protein and cytochrome c_1. Then, the second electron of ubiquinol, via a transient semiquinone, is passed through the "low potential chain," consisting of cytochromes b_L and b_H, to reduce ubiquinone or ubisemiquinone bound at the ubiquinol reduction site (Q_N). One drawback of this sequential scheme is the lack of a "functional" semiquinone at the ubiquinol oxidation site (Q_P) (12–14), even though some radicals have been reported under abnormal conditions (15, 16). Recently, pre-steady-state kinetic analysis of the reduction of cytochrome b_L and the Rieske iron-sulfur protein in the same sample using fast quenching coupled with EPR (17) indicated that both the iron-sulfur cluster and heme b_L are reduced by ubiquinol at the same rate, suggesting a concerted scheme for the bifurcated oxidation of ubiquinol at the Q_P site (18, 19).

It has been established that for every electron transferred through the bc_1 complex, two protons are translocated across the membrane. This $2H^+/e^-$ stoichiometry has been verified in a wide variety of species through *in vitro* studies of bc_1 complexes in phospholipid (PL)[2] vesicles.

Arg-79 in cytochrome *b* of the yeast bc_1 complex is hydrogen-bonded to the heme propionate and provides a proton exit pathway to the bulk solvent mediated by a chain of hydrogen-bonded water molecules. Arg-79 is fully conserved in cytochrome *b*, indicating its importance for the catalytic mecha-

[*] This work was supported, in whole or in part, by National Institutes of Health Grant GM30721 (to C.-A. Y.). This work was also supported by National Science Foundation Grant MCB0077650 (to L. Y.) and Oklahoma Agricultural Experiment Station Projects 1819 and 2372 from Oklahoma State University.

[1] To whom correspondence should be addressed: Dept. of Biochemistry and Molecular Biology, 255 Noble Research Center, Oklahoma State University, Stillwater, OK 74078. E-mail: yuangangqu@yahoo.com.

[2] The abbreviations used are: PL, phospholipid; CCCP, carbonyl cyanide *m*-chlorophenylhydrazone; MCLA, 2-methyl-6-(4-methoxyphenyl)-3,7-dihydroimidazo[1,2-α]pyrazin-3-one hydrochloride; $Q_0C_{10}BrH_2$, 2,3-dimethoxy-5-methyl-6-(10-bromodecyl)-1,4-benzoquinol.

TABLE 1

Oligonucleotides used for site-directed mutagenesis

The underlined bases correspond to the genetic codes for the amino acid(s) to be mutated.

Primer	Sequence
R94A	
Forward	GCTTCATGCTGGCCTACCTGCATGCG
Reverse	CGCATGCAGGTAGGCCAGCATGAAGC
R94N	
Forward	GCTTCATGCTGAACTACCTGCATGCG
Reverse	CGCATGCAGGTAGTTCAGCATGAAGC
R94D	
Forward	GCTTCATGCTGGACTACCTGCATGCG
Reverse	CGCATGCAGGTAGTCCAGCATGAAGC

nism (20). Arg-94 in cytochrome *b* of *Rhodobacter sphaeroides* corresponds to Arg-79 in yeast. To further elucidate the role of this important amino acid in cytochrome *b* of *R. sphaeroides*, we report herein detailed procedures for generating mutations of Arg-94 in cytochrome *b* and characterize the electron transfer activity, proton pumping capability, pre-steady-state reduction kinetics of hemes (*b* and c_1), and superoxide anion production in purified bc_1 complexes. We found that substitution of Arg-94 decreased electron transfer activity and proton pumping capability and increased superoxide anion production. The transport of H^+, O_2, and O_2^- may follow the same pathway.

EXPERIMENTAL PROCEDURES

Materials—Cytochrome *c* (horse heart, type III), stigmatellin, antimycin A, carbonyl cyanide *m*-chlorophenylhydrazone (CCCP), and valinomycin were purchased from Sigma. 8-Hydroxypyrene-1,3,6-trisulfonic acid trisodium salt (pyranine) was from Acros Organics. Asolectin was obtained from Associated Concentrates and purified according to the method of Kagawa and Racker (21). *n*-Dodecyl-β-D-maltopyranoside and *n*-octyl-β-D-glucopyranoside were from Anatrace. Nickel-nitrilotriacetic acid gel, a QIAprep spin miniprep kit, and a PCR purification kit were obtained from Qiagen. 2-Methyl-6-(4-methoxyphenyl)-3,7-dihydroimidazo[1,2-α]pyrazin-3-one hydrochloride (MCLA) was from Molecular Probes. 2,3-Dimethoxy-5-methyl-6-(10-bromodecyl)-1,4-benzoquinol ($Q_0C_{10}BrH_2$) was prepared in our laboratory as reported previously (22). All other chemicals were of the highest purity commercially available.

Generation of R. sphaeroides Cytochrome bc_1 Mutants—Mutations were constructed using the QuikChange site-directed mutagenesis kit (Stratagene) with supercoiled double-stranded pGEM7Zf(+)-*fbc*B as a template. Forward and reverse primers were used for PCR amplification (Table 1). The pGEM7Zf(+)-*fbc*B plasmid (23) was constructed by ligating the NsiI-XbaI fragment from pRKD418-*fbc*FB_{6H}Q into the NsiI and XbaI sites of the pGEM7Zf(+) plasmid. The NsiI-XbaI fragment from the pGEM7Zf(+)-*fbc*B_m plasmid was ligated into the NsiI and XbaI sites of the pRKD418-*fbc*FBK_mC_{6H}Q plasmid to generate the pRKD418-*fbc*FB_mC_{6H}Q plasmid. A plate-mating procedure (24) was used to mobilize the pRKD418-*fbc*FB_mC_{6H}Q plasmid in *Escherichia coli* S17 cells into *R. sphaeroides* BC17 cells. The presence of the engineered mutations was confirmed by DNA sequencing before and after semi-aerobic growth of the cells. The expression plasmid pRKD*fbc*F$_mBC_H$Q was purified from an aliquot of semi-aerobically grown culture using the Qiagen plasmid miniprep kit. Because *R. sphaeroides* cells contain four types of endogenous plasmids, the isolated plasmids lacked the purity and concentration needed for direct sequencing. Therefore, a 2-kilobase pair DNA segment containing the mutation sequence was amplified from the isolated plasmids by PCR. The PCR products were purified with an extraction kit from Sigma and then sequenced. DNA primers were purchased from Invitrogen. DNA sequencing was carried out at the Recombinant DNA/Protein Core Facility of Oklahoma State University.

Growth of Bacteria—E. coli cells were grown at 37 °C in LB medium. *R. sphaeroides* BC17 cells (24) were grown photosynthetically at 30 °C in enriched Siström's medium containing 5 mM glutamate and 0.2% casamino acids. Photosynthetic growth conditions for *R. sphaeroides* were essential as described previously (25). The concentrations and antibiotics used were as follows: ampicillin, 125 μg/ml; kanamycin sulfate, 30 μg/ml; tetracycline, 10 μg/ml for *E. coli* and 1 μg/ml for *R. sphaeroides*; and trimethoprim, 100 μg/ml for *E. coli* and 30 μg/ml for *R. sphaeroides*.

Enzyme Preparations and Specific Electron Transfer Activity Assay—Chromatophore membranes were prepared from frozen cell paste, and cytochrome bc_1 complexes with a His_6 tag placed at the C terminus of cytochrome c_1 were purified from chromatophores as described previously (25) and stored at −80 °C in the presence of 10% glycerol. Protein concentrations were determined by absorbance at 280 nm using a converting factor of 1 A_{280} = 0.56 mg/ml. The concentrations of cytochromes *b* and c_1 were determined spectrophotometrically using published molar extinction coefficients (26–28).

To assay ubiquinol-cytochrome *c* reductase activity, purified cytochrome bc_1 complexes were diluted with 50 mM Tris-Cl (pH 8.0) containing 200 mM NaCl and 0.01% *n*-dodecyl-β-D-maltopyranoside to a final cytochrome *b* concentration of 1 μM unless specified otherwise. Appropriate amounts of the diluted samples were added to 1 ml of assay mixture containing 100 mM Na^+/K^+ phosphate buffer (pH 7.4), 0.3 mM EDTA, 100 μM cytochrome *c*, and 25 μM $Q_0C_{10}BrH_2$. The specific electron transfer activities were determined by measuring the reduction of cytochrome *c* (the increase in the absorbance at a wavelength of 550 nm) with a Shimadzu UV-2401 PC spectrophotometer at 23 °C using a millimolar extinction coefficient of 18.5 for calculation. The non-enzymatic oxidation of $Q_0C_{10}BrH_2$, determined under the same conditions in the absence of enzyme, was subtracted during specific activity calculations. Although the chemical properties of $Q_0C_{10}BrH_2$ are comparable with those of $Q_0C_{10}H_2$, the former is a better substrate for the cytochrome bc_1 complex (22).

Preparation of Electron Transfer Complex-inlaid PL Vesicles—Protein-PL vesicles were prepared by the cholate dialysis method of Kagawa and Racker (21). The wild-type or mutant bc_1 complex was mixed with 1 ml of asolectin micellar solution to give an asolectin (milligrams)/protein (milligrams) ratio of 40. The asolectin micellar solution was prepared by sonicating 200 mg of acetone-washed asolectin in 4 ml of 50 mM sodium phosphate buffer (pH 7.4) containing 2% sodium cholate and 100 mM KCl in an ice-water bath. Sonication was performed in

an anaerobic environment by continually passing argon into the vessel. The bc_1 complex/PL mixtures were incubated at 0 °C for 30 min before overnight dialysis at 4 °C against 100 volumes of 50 mM sodium phosphate buffer (pH 7.4) containing 100 mM KCl with three changes of buffer. The mixture was then dialyzed against 100 volumes of 150 mM KCl for 3–4 h.

Determination of Proton Translocation Activity of bc_1 Complex-PL Vesicles—Proton translocation coupled to electron flow through the bc_1 complex-PL vesicles was measured at room temperature using an Accumet Model 10 pH meter and Model 13-620-96 combination pH electrode. 25 nmol of $Q_0C_{10}BrH_2$ was added to the 1.6-ml reaction mixture containing 150 mM KCl, 4 μM ferricytochrome *c*, 1 μM valinomycin, and an appropriate amount of bc_1 complex-PL vesicles (30–50 μl). Electron flow was initiated by the addition of 5 nmol of ferricyanide, which oxidizes the cytochrome *c* and thus provides an electron acceptor for the complex. Electron flow under conditions in which no transmembrane ΔpH formed was measured in an identical manner except that the protonophore CCCP was present at a concentration of 2 μM to make the vesicles permeable to protons. Proton pumping (H^+/e^-) was calculated as the ratio of the decrease in pH upon ferricyanide addition to bc_1 complex-PL vesicles before and after treatment with CCCP.

Fast Kinetics Study—Measurements were performed in an Applied Photophysics SX.18MV stopped-flow spectrometer with a photodiode array scan between 600 and 500 nm. The reaction was started by mixing equal volumes of solutions A and B at room temperature. For the experiment to determine electron transfer rates between ubiquinol and heme *b* or c_1, solution A contained 50 mM Tris-Cl (pH 8.0) at 4 °C, 200 mM NaCl, 0.01% *n*-dodecyl-β-D-maltopyranoside, and 12.0 μM cytochrome bc_1 complex (based on cytochrome c_1). Solution B was the same as solution A except that the bc_1 complex was replaced with 240 μM $Q_0C_{10}BrH_2$. Reductions of cytochromes *b* and c_1 were determined from the absorption changes at 560–580 nm and at 551–539 nm, respectively. When an inhibitor was used, the cytochrome bc_1 complex was treated with a 5-fold molar excess of inhibitor over heme c_1 for 5 min at 4 °C prior to the experiment.

Because the concentration of ubiquinol used was much higher than that of the cytochrome bc_1 complex, the reactions between bc_1 and ubiquinol were treated as pseudo first-order reactions. Time traces of the reaction were fitted using a first-order rate equation to obtain the pseudo first-order rate constants (k_1) by KaleidaGraph.

For the experiment to determine proton production rates, solution A contained 150 mM KCl, 30 μM $Q_0C_{10}BrH_2$, 2 μM valinomycin, 100 μM pyranine, and bc_1 complex-PL vesicles (35 μl/ml of solution A). Solution B contained 150 mM KCl and 8 μM ferricytochrome *c*. Solutions A and B were both adjusted carefully to pH 7.0 with 2 mM KOH. Proton pumping was determined from the absorption changes at 457 nm.

Measurement of Superoxide Anion Generation—Superoxide anion generation by the cytochrome bc_1 complex was determined by measuring the chemiluminescence of the MCLA-O_2^- adduct (29) in an Applied Photophysics SX.18MV stopped-flow spectrometer by leaving the excitation light off and registering the light emission (30). Reactions were carried out at 23 °C by mixing solutions A and B at 1:1. Solution A contained 100 mM Na^+/K^+ phosphate buffer (pH 7.4), 1 mM EDTA, 1 mM KCN, 1 mM NaN_3, 0.1% bovine serum albumin, 0.01% *n*-dodecyl-β-D-maltopyranoside, and 5.0 μM wild-type or mutant bc_1 complex. Solution B was the same as solution A except that the bc_1 complex was replaced with 150 μM $Q_0C_{10}BrH_2$ and 4 μM MCLA.

TABLE 2
Characterization of mutants
The cytochrome bc_1 complexes were in 50 mM Tris-Cl (pH 8.0) containing 200 mM NaCl, 200 mM histidine, 0.5% octyl glucoside, and 10% glycerol.

Strain	Photosynthetic growth	Activity[a]
WT	++++	4.58 (100%)
R94A	+	0.18 (4%)
R94D	++	1.61 (35%)
R94N	+++	2.34 (51%)

[a] The enzyme-specific electron transfer activity of the purified bc_1 complexes is expressed as micromoles of cytochrome *c* reduced per min/nmol of cytochrome *b* at room temperature.

RESULTS AND DISCUSSION

Photosynthetic Growth Behaviors of the Wild-type and Mutant bc_1 Complexes—Because the cytochrome bc_1 complex is absolutely necessary for photosynthetic growth of *R. sphaeroides*, a mutant with a substitution at a critical position will not grow photosynthetically, whereas mutants with substitutions at noncritical positions will grow. Thus, observing the photosynthetic growth behavior, one can determine whether substitutions are at critical positions. In mid-log phase, semiaerobically dark-grown wild-type and mutant cells were inoculated into enriched Siström's medium and subjected to anaerobic photosynthetic growth conditions. Table 2 shows that mutants could grow, indicating that substitutions of Arg-94 are noncritical to the complex. These mutants grew at a decreased rate compared with the wild-type bc_1 complex, suggesting that substitutions of Arg-94 affect the function of the cytochrome bc_1 complex and thus retard the growth of *R. sphaeroides*.

Proton Translocation Activity of the Wild-type and Mutant bc_1 Complexes—The bc_1 complex catalyzes electron transfer from ubiquinol to cytochrome *c* and concomitantly translocates protons of ubiquinol across the membrane. The two protons of ubiquinol are released via two pathways. The ejection of the first proton is controlled by the protonation and deprotonation of the histidine ligands of the [2Fe-2S] cluster. The histidine ligands take up a proton from the substrate, ubiquinol, upon reduction of the [2Fe-2S] cluster and release it to the intermembrane space when oxidized by cytochrome c_1, as was suggested recently (31). Glu-295 in cytochrome *b* is important for the release of the second proton, as proposed previously (31–33). Glu-295 is completely conserved in mitochondrial cytochrome *b* (34), and the importance of the residue in proton transfer is indicated by mutagenesis studies because alteration of glutamine abolishes ubiquinol oxidation in *R. sphaeroides* (35). Additionally, recent kinetic studies showed that protonation of a group with a pK_a of 5.7 blocked catalysis, and this effect was attributed to Glu-295 (36). The second proton of ubiquinol is first transferred to Glu-295 to form the neutral acid and is then released and delivered to heme propionate A by rotation of the side chain of Glu-295. The subsequent proton release is mediated by a hydrogen-bonded water chain stabilized by cytochrome *b* residues (Fig. 1) (20, 31).

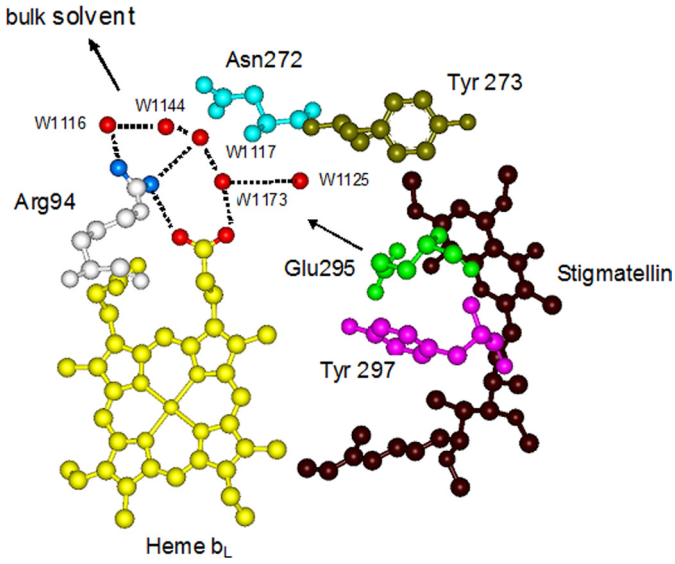

FIGURE 1. **Proton exit pathway formed by a chain of hydrogen-bonded water molecules at the Q_P site with the stigmatellin bound.** *Blue dots* on Arg-94 indicate the NH_1 and NH_2 groups. *Red dots* on heme b_L indicate O1A and O2A. Other *red dots* indicate water (*W*) molecules. The *arrow* shows the proton exit pathway from Glu-295 to bulk solvent.

The proton pumping property has been well demonstrated in PL vesicles embedded with the purified mitochondrial bc_1 complex (37–40). Fig. 2 shows a typical proton translocation activity assay for PL vesicles embedded with the *R. sphaeroides* bc_1 complex. After pH equilibrium was reached for the mixture containing $Q_0C_{10}BrH_2$, valinomycin, ferricytochrome *c*, and bc_1 complex-PL vesicles, an aliquot of ferricyanide solution (*arrow 1*) was added to initiate electron flow from $Q_0C_{10}BrH_2$ to cytochrome *c*. After pH equilibrium was attained, the protonophore CCCP was added (*arrow 2*) to render the liposome membrane freely permeable to protons, and then a second aliquot of ferricyanide was added (*arrow 3*). The ratio of the pH changes produced by the addition of equal amounts of ferricyanide before (*x*) and after (*y*) the addition of CCCP was taken as a measure of the H^+/e^- ratio for the proton translocation activity of the bc_1 complex. The protons released after CCCP addition were the "scalar" protons only, as no contribution from the accumulation of "vectorially" translocated protons was possible.

Table 3 shows the proton translocation activity (H^+/e^-) of the wild-type and mutant bc_1 complexes. The proton translocation activity of R94N showed a small decrease compared with the wild-type bc_1 complex, whereas that of R94A and R94D exhibited a significant decrease. H^+/e^- reflects only the final ratio of proton translocation to electron transfer. To further study the proton translocation rate, a kind of dye, pyranine, was used in a stopped-flow experiment. Fig. 3 shows that the magnitude of proton translocation rate of the wild-type and mutant bc_1 complexes can be ranked as WT > R94N > R94D > R94A. These results indicate that a positive correlation exists between the changes in proton translocation activity (H^+/e^-) and the proton translocation rate.

Proton transfer pathways involving internal water molecules that provide hydrogen bonds and facilitate proton diffusion have been identified in other membrane proteins such as bacteriorhodopsin (41) and cytochrome *c* oxidase (42). Although the mechanisms for proton translocations are different for different proteins, the underlying principle for bringing protons to the active sites is similar. For Arg-94, the nitrogen atom of the guanidyl easily forms a hydrogen bond with H_2O, and the repulsion function of the positive charge to H^+ is also favorable for H^+ movement. For Ala, the carbon atom of the methyl does not easily form a hydrogen bond with H_2O, and there is no positive charge on its side chain. In addition, as a hydrophobic amino acid, the hydrophobic microenvironment is also unfavorable

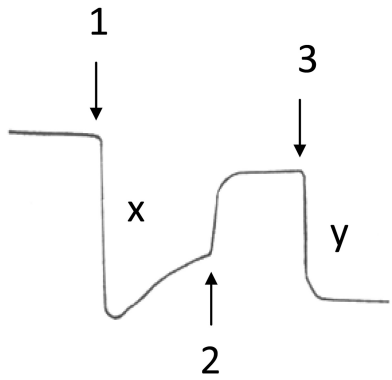

FIGURE 2. **Proton pumping of *R. sphaeroides* cytochrome bc_1 complexes embedded in PL vesicles.** *Arrows* indicate the points of addition of 5 nmol of ferricyanide (*arrow 1*), 2 μM CCCP (*arrow 2*), and 5 nmol of ferricyanide (*arrow 3*). Note that the proton pumping ratio (H^+/e^-) = *x*/*y*.

TABLE 3

Proton pumping ratios (H^+/e^-) for PL vesicles harboring wild-type and mutant bc_1 complexes

For the definition of H^+/e^- and experimental conditions, see "Experimental Procedures" and the legend to Fig. 2.

Vesicle type	H^+/e^-
WT	1.5
R94A	1.2
R94D	1.23
R94N	1.48

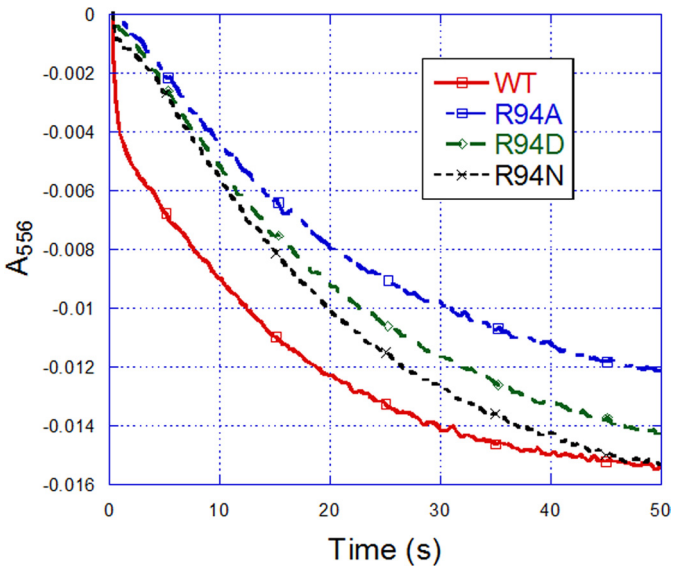

FIGURE 3. **Determination of proton translocation rate of PL vesicles embedded with wild-type or mutant bc_1 complexes using a stopped-flow spectrophotometer.** Reaction conditions were as described under "Experimental Procedures." pH changes were monitored by following the absorption change of pyranine at 457 nm.

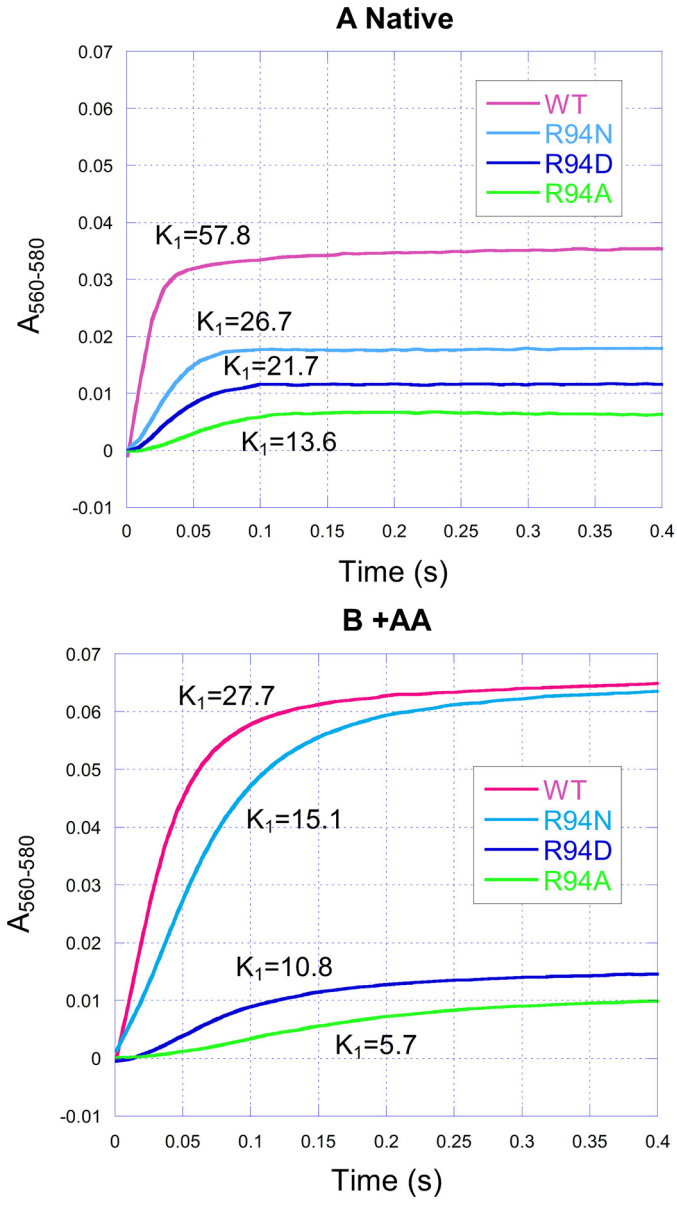

FIGURE 4. **Time traces of cytochrome *b* reduction by $Q_0C_{10}BrH_2$ in the wild-type and mutant complexes in the absence (*A*) and presence (*B*) of antimycin A.** Reactions and measurements were performed as described under "Experimental Procedures." The reaction was monitored by photodiode array scanning for 0.4 s. Cytochrome *b* was determined from the increase in $A_{560-580}$. *AA*, antimycin A.

for H^+ movement. Thus, the proton translocation activity of the R94A mutant is inhibited. The structure of Asn is similar to that of Arg except for a small difference in molecular weight, so the proton translocation activity of the R94N mutant is similar to that of the wild type. The low proton translocation activity of R94D may be due to the negative charge of the side chain of Asp exerting an attractive force to H^+, which is unfavorable for H^+ movement. The low proton translocation activity of the mutants indicates that some of the "second H^+" of $Q_0C_{10}BrH_2$ cannot be pumped into the exterior of the vesicle and also suggests that Arg-94 in cytochrome *b* of the bc_1 complex is an important amino acid for proton pumping.

Effect of Mutations on Cytochrome b Reduction by Ubiquinol—Fig. 4 shows the time course traces of heme *b* reduction by $Q_0C_{10}BrH_2$ in the wild type and mutants in the absence (*panel A*) and presence (*panel B*) of antimycin A. Antimycin A is a Q_N site inhibitor that blocks electron transfer from heme b_H to ubiquinone and prevents reduction of heme b_H by $Q_0C_{10}BrH_2$ through the Q_N site.

In the case of the native complex (Fig. 4*A*), the extent of heme *b* reduction of mutants decreased relative to the wild type. It should be noted that heme *b* reduction is mostly heme b_H (43). The heme b_H reduction by ubiquinol in the bc_1 complex, according to the Q-cycle mechanism, is affected by (i) the forward reduction through the Q_P site to heme b_L and then to b_H, (ii) the reoxidation of reduced heme b_H by ubiquinone, and (iii) the "back door" reduction through the Q_N site. Therefore, it is difficult to explain the differences in the extent of heme *b* reduction among the wild type and mutants.

In the presence of antimycin A (Fig. 4*B*), heme *b* reduction by $Q_0C_{10}BrH_2$ occurred only through the Q_P site via heme b_L, so this case is simplified. Relative to the wild type, the heme *b* reduction extent of R94N, R94D, and R94A decreased by 2.4, 77.71, and 84.93%, respectively. This decrease implies that some electrons may deviate from the low potential electron transfer chain and leak from the reduced heme b_L or ubisemiquinone at the Q_P site during bc_1 catalysis. The results also indicate that the extent of the electron leak is WT < R94N < R94D < R94A.

Whether in the absence or presence of antimycin A, the rate constants of heme *b* reduction of the mutants all decreased relative to the wild type, and the extent of the decrease can be described as R94N < R94D < R94A (Fig. 4). The decrease in the rate constants of heme *b* reduction suggests that the transfer rate of the second electron of $Q_0C_{10}BrH_2$ is decreased for mutants.

The addition of antimycin A (Fig. 4) increased the extent and decreased the rate of heme *b* reduction in the wild type and mutants, and these results are consistent with a previous report (44). However, the degree of this effect varied in these complexes. Relative to the native case (Fig. 4*A*), the rate of heme *b* reduction of the wild type, R94N, R94D, and R94A was decreased by 52, 43, 50, and 58%, respectively. Relative to the native case (Fig. 4*A*), the extent of heme *b* reduction of the wild type, R94N, R94D, and R94A was increased by 83, 255, 25, and 56%, respectively.

Effect of Mutations on Cytochrome c_1 Reduction by Ubiquinol—Fig. 5 shows the time course traces of heme c_1 reduction by $Q_0C_{10}BrH_2$ in the wild type and mutants in the absence (*panel A*) and presence (*panel B*) of antimycin A. In both the absence and presence of antimycin A, the rate constants of heme c_1 reduction of all mutants decreased relative to the wild type, and the extent of the decrease is R94N < R94D < R94A. The decrease in the rate constants of heme c_1 reduction suggests that the transfer rate of the first electron of $Q_0C_{10}BrH_2$ is decreased for mutants.

Relative to the values for the native case, the addition of antimycin A decreased the rate of heme c_1 reduction by 18, 9, 9, and 73% in the wild type, R94N, R94D, and R94A, respectively (Fig. 5). These results are consistent with previous reports (18, 43) that antimycin A has a significant effect on the reduction rate of heme c_1 in cytochrome bc_1 complexes. This inhibitive effect has

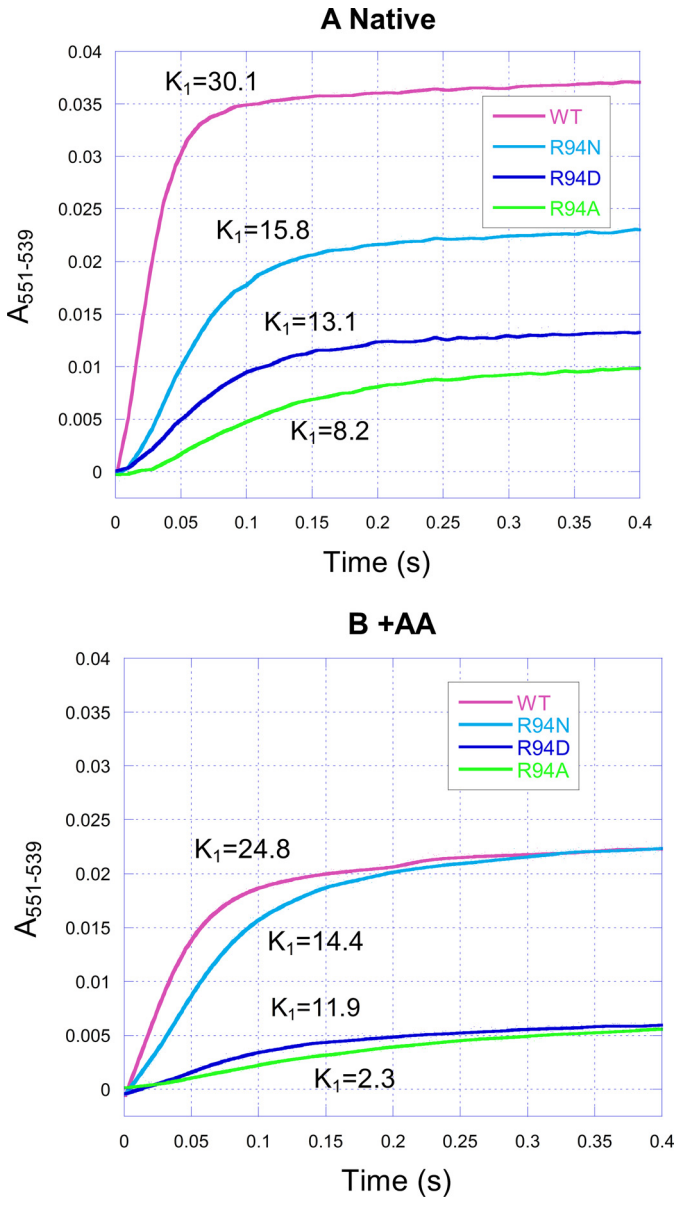

FIGURE 5. **Time traces of cytochrome c_1 reduction by $Q_0C_{10}BrH_2$ in the wild-type and mutant complexes in the absence (*A*) and presence (*B*) of antimycin A.** Reactions and measurements were performed as described under "Experimental Procedures." The reaction was monitored by photodiode array scanning for 0.4 s. Cytochrome c_1 was determined from the increase in $A_{551-539}$. *AA*, antimycin A.

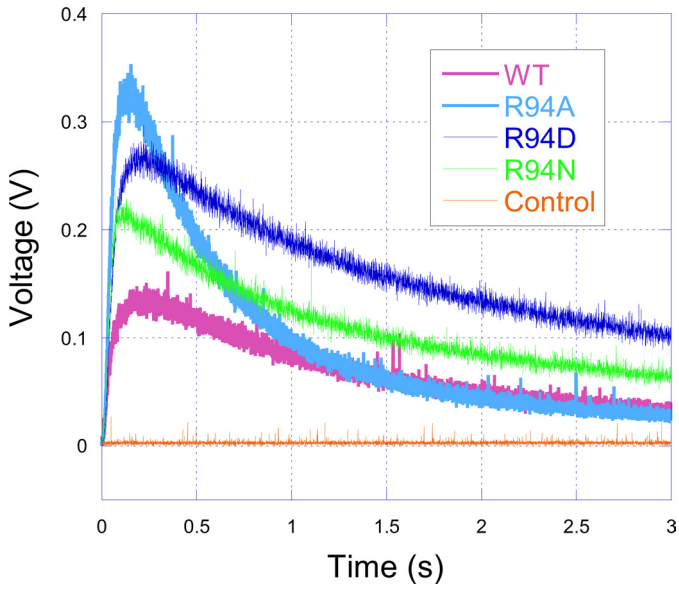

FIGURE 6. **Time traces of superoxide anion generation.** The superoxide anion generation reactions were carried out at 23 °C in an Applied Photophysics SX.18MV stopped-flow reaction analyzer by mixing solutions A and B (1:1) containing enzyme complexes and substrate as described under "Experimental Procedures." The *orange trace* is for control experiments, when no bc_1 complexes were present in the system.

been attributed to the long-range effect of antimycin A on the Q_P site when binding to the Q_N site (18, 43). In other words, the effect of antimycin A on the heme c_1 reduction rate does not occur through the low potential redox component but through the cytochrome *b* protein subunit.

In the Q-cycle mechanism, the oxidation of ubiquinol and reduction of ubiquinone or ubisemiquinone occur mainly in the Q_P and Q_N sites of cytochrome *b*. In the mutant bc_1 complexes, the Q_P and Q_N sites are functional because all of the mutant complexes were sensitive to antimycin A (Figs. 4*B* and 5*B*) and stigmatellin (a Q_P site inhibitor) (data not shown). The changes in electron transfer activity or the changes in heme *b* and c_1 reduction should all be related to the mutation at Arg-94, but they are not related to the impairment of the Q_P or Q_N site.

Substitution of Arg-94 decreased the proton translocation rate, slowed down the decomposition rate of $Q_0C_{10}BrH_2$ by feedback inhibition, and then slowed down the transfer of the two electrons of ubiquinol. A decrease in the first electron transfer induced the heme c_1 reduction rate decrease and the electron transfer activity decrease (Table 2). A decrease in the second electron transfer induced the heme *b* reduction rate decrease (Fig. 4).

The decreases in the proton translocation rate, the heme *b* and c_1 reduction rate, and the electron transfer activity all changed in the same order of R94N < R94D < R94A for the three mutants. This positive correlation also supports the relationship discussed above. In addition, the decreases in the heme *b* reduction rate and the electron transfer activity are also related to the production of superoxide anion, as discussed below.

Effect of Mutations on Superoxide Anion Production by the Cytochrome bc_1 Complex—The above results show that some electrons may leak from the low potential electron transfer chain during bc_1 catalysis for mutants. What is the fate of these leaked electrons? One of the possible pathways is a reaction with molecular oxygen to form superoxide anions. If this is the pathway, one should see more superoxide anion production by mutants than the wild-type complex because more electrons leak from the mutant complexes.

Fig. 6 shows the tracings of $O_2^{\cdot-}$ generation by the wild type and mutants. MCLA-$O_2^{\cdot-}$ chemiluminescence induced by the bc_1 complex reached peak intensity after ~0.1 s at room temperature and then decayed. Relative to the wild type, $O_2^{\cdot-}$ generation increased by 18, 36, and 61% for R94N, R94D, and R94A, respectively. No luminescence was detected when the bc_1 complex was omitted from the enzyme-containing solution. This result suggests that some electrons do leak from the low potential electron transfer chain to O_2 and then form $O_2^{\cdot-}$ during bc_1

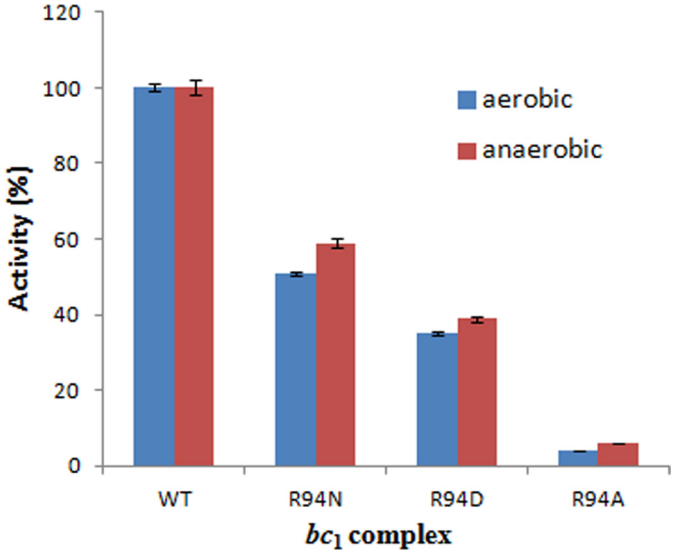

FIGURE 7. **Electron transfer activity changes in the wild-type and mutant complexes under aerobic and anaerobic conditions.** The activity of the wild type is regarded as 100%, and that of mutants is described as the percentage of the wild type. Data represent an average of three experiments. *Error bars* indicate S.D. The difference is significant ($p < 0.05$, Student's *t* test) between aerobic and anaerobic conditions for every mutant complex.

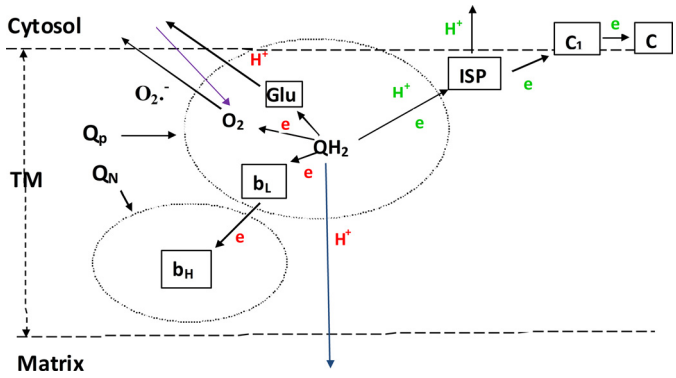

FIGURE 8. **Schematic depiction of the transfer of the two electrons and two protons of ubiquinol at the Q_P pocket when it is oxidized in the bc_1 complex.** The first electron and proton are in *green*, and the second electron and proton are in *red*. The *blue arrow* indicates protons that return to the matrix for mutants; the *purple arrow* indicates oxygen molecules that are transferred to the Q_P quinol oxidation pocket from the cytosol solvent. Q_N is the quinone reduction pocket. *QH_2*, ubiquinol; *TM*, transmembrane region; *ISP*, Rieske iron-sulfur protein.

catalysis. The result also indicates that the extent of the electron leak is WT < R94N < R94D < R94A, which is the same as the result from the heme *b* reduction analysis above. There is an inverse relationship between $O_2^{\cdot-}$ production and the heme *b* reduction rate (Figs. 4 and 6). The heme *b* reduction rate indicates the second electron transfer rate. It can therefore be deduced that another reason for the decreased second electron transfer rate in the hydrophobic Q_P pocket for mutants is the increased $O_2^{\cdot-}$ production. More superoxide anions released means a lower electron transfer rate.

In addition, the generation of more $O_2^{\cdot-}$ implies that more electrons are consumed by O_2 in the bc_1 complex, which would result in decreased electron transfer activity. Thus, the decreased activity of mutants is ascribed to the increased $O_2^{\cdot-}$ generation as well as to the decreased proton pumping (discussed above). Under anaerobic conditions, there is no $O_2^{\cdot-}$ generation. Thus, one can deduce that the difference between activities in a mutant and the wild type under anaerobic conditions should be less than that under aerobic conditions. This is indeed the case. Fig. 7 shows that, compared with the wild type, the electron transfer activities of R94N, R94D, and R94A decreased by 49, 65, and 96%, respectively, under aerobic conditions, whereas they decreased by 41, 61, and 94%, respectively, under anaerobic conditions. The difference is significant ($p < 0.05$, Student's *t* test) between aerobic and anaerobic conditions for every mutant complex. These data also show that the effect of the superoxide anion generation on the decrease in the electron transfer activity of mutants is R94N > R94D > R94A, and the superoxide anion generation has a smaller effect on the decrease in the electron transfer activity of mutants compared with the proton pumping decrease.

Transport Pathway of H^+, O_2, and $O_2^{\cdot-}$ in the bc_1 Complex—It is known that $O_2^{\cdot-}$ is generated inside the bc_1 complex, perhaps in the hydrophobic environment of the Q_P pocket through bifurcated oxidation of ubiquinol by transfer of its two electrons to a high potential electron acceptor, an iron-sulfur cluster, and a low potential heme b_L or molecular oxygen. The protein subunits, at least those surrounding the Q_P pocket, play a role either in preventing the release of $O_2^{\cdot-}$ from its production site to aqueous environments or in preventing O_2 from getting access to the hydrophobic Q_P pocket (45). The increase in superoxide anion production by mutants (Fig. 6) may result from the rapid transport of O_2 and $O_2^{\cdot-}$ between the hydrophobic Q_P pocket and the aqueous phase because the O_2 concentrations in the aqueous phase of the wild type and mutants are the same.

Substitution of Arg-94 changes the proton pumping and $O_2^{\cdot-}$ generation simultaneously. This suggests that the transport of H^+, O_2, and $O_2^{\cdot-}$ may occur by the same pathway as described in Figs. 1 and 8. Arg-94 of cytochrome *b* may function as a gate for the transport of H^+, O_2, and $O_2^{\cdot-}$. However, the factors that influence the transport of H^+, O_2, and $O_2^{\cdot-}$ may be different. H^+ transport is related mainly to the hydrogen bond and charge as described above, whereas that of O_2 and $O_2^{\cdot-}$ may be affected mainly by the side chain size of Arg-94 or its substitute. The long side chain, *e.g.* that of Arg-94 in the wild type, is unfavorable for the movement of O_2 and $O_2^{\cdot-}$, and this results in low $O_2^{\cdot-}$ production. However, a short side chain, *e.g.* that of Ala-94, is favorable for the movement of O_2 and results in high $O_2^{\cdot-}$ production. In addition, as a hydrophobic amino acid of Ala, the hydrophobic environment is also favorable to the solubility of O_2 and generation of $O_2^{\cdot-}$ (45). More $O_2^{\cdot-}$ production by R94D than R94N may be related to the negative charge, which has a repellent force to $O_2^{\cdot-}$, providing a favorable condition for $O_2^{\cdot-}$ movement. In this study, only one residue was mutated and studied, so this suggestion remains to be further investigated.

REFERENCES

1. Bartoschek, S., Johansson, M., Geierstanger, B. H., Okun, J. G., Lancaster, C. R., Humpfer, E., Yu, L., Yu, C.-A., Griesinger, C., and Brandt, U. (2001) Three molecules of ubiquinone bind specifically to mitochondrial cytochrome bc_1 complex. *J. Biol. Chem.* **276,** 35231–35234
2. Trumpower, B. L., and Gennis, R. B. (1994) Energy transduction by cytochrome complexes in mitochondrial and bacterial respiration: the enzymology of coupling electron transfer reactions to transmembrane proton

translocation. *Annu. Rev. Biochem.* **63,** 675–716
3. Xia, D., Yu, C.-A., Kim, H., Xia, J. Z., Kachurin, A. M., Zhang, L., Yu, L., and Deisenhofer, J. (1997) Crystal structure of the cytochrome bc_1 complex from bovine heart mitochondria. *Science* **277,** 60–66
4. Iwata, S., Lee, J. W., Okada, K., Lee, J. K., Iwata, M., Rasmussen, B., Link, T. A., Ramaswamy, S., and Jap, B. K. (1998) Complete structure of the 11-subunit bovine mitochondrial cytochrome bc_1 complex. *Science* **281,** 64–71
5. Zhang, Z., Huang, L., Shulmeister, V. M., Chi, Y. I., Kim, K. K., Hung, L. W., Crofts, A. R., Berry, E. A., and Kim, S. H. (1998) Electron transfer by domain movement in cytochrome bc_1. *Nature* **392,** 677–684
6. Erecińska, M., Chance, B., Wilson, D. F., and Dutton, P. L. (1972) Aerobic reduction of cytochrome b_{566} in pigeon-heart mitochondria. *Proc. Natl. Acad. Sci. U.S.A.* **69,** 50–54
7. Wikström, M. K., and Berden, J. A. (1972) Oxidoreduction of cytochrome *b* in the presence of antimycin. *Biochim. Biophys. Acta* **283,** 403–420
8. Alexandre, A., and Lehninger, A. L. (1979) Stoichiometry of H^+ translocation coupled to electron flow from succinate to cytochrome *c* in mitochondria. *J. Biol. Chem.* **254,** 11555–11560
9. Mitchell, P. (1976) Possible molecular mechanisms of the protonmotive function of cytochrome systems. *J. Theor. Biol.* **62,** 327–367
10. Brandt, U., and Trumpower, B. (1994) The protonmotive Q cycle in mitochondria and bacteria. *Crit. Rev. Biochem. Mol. Biol.* **29,** 165–197
11. Crofts, A. R. (2004) The cytochrome bc_1 complex: function in the context of structure. *Annu. Rev. Physiol.* **66,** 689–733
12. Link, T. A. (1997) The role of the 'Rieske' iron sulfur protein in the hydroquinone oxidation (Q_P) site of the cytochrome bc_1 complex: the 'proton-gated affinity change' mechanism. *FEBS Lett.* **412,** 257–264
13. Jünemann, S., Heathcote, P., and Rich, P. R. (1998) On the mechanism of quinol oxidation in the bc_1 complex. *J. Biol. Chem.* **273,** 21603–21607
14. Zhang, H., Osyczka, A., Dutton, P. L., and Moser, C. C. (2007) Exposing the complex III Q_o semiquinone radical. *Biochim. Biophys. Acta* **1767,** 883–887
15. de Vries, S., Albracht, S. P., Berden, J. A., and Slater, E. C. (1981) A new species of bound ubisemiquinone anion in QH_2:cytochrome *c* oxidoreductase. *J. Biol. Chem.* **256,** 11996–11998
16. Cape, J. L., Bowman, M. K., and Kramer, D. M. (2007) A semiquinone intermediate generated at the Q_o site of the cytochrome bc_1 complex: importance for the Q-cycle and superoxide production. *Proc. Natl. Acad. Sci. U.S.A.* **104,** 7887–7892
17. Zhu, J., Egawa, T., Yeh, S.-R., Yu, L., and Yu, C.-A. (2007) Simultaneous reduction of iron-sulfur protein and cytochrome b_L during ubiquinol oxidation in cytochrome bc_1 complex. *Proc. Natl. Acad. Sci. U.S.A.* **104,** 4864–4869
18. Snyder, C. H., Gutierrez-Cirlos, E. B., and Trumpower, B. L. (2000) Evidence for a concerted mechanism of ubiquinol oxidation by the cytochrome bc_1 complex. *J. Biol. Chem.* **275,** 13535–13541
19. Crofts, A. R., Holland, J. T., Victoria, D., Kolling, D. R., Dikanov, S. A., Gilbreth, R., Lhee, S., Kuras, R., and Kuras, M. G. (2008) The Q-cycle reviewed: how well does a monomeric mechanism of the bc_1 complex account for the function of a dimeric complex? *Biochim. Biophys. Acta* **1777,** 1001–1019
20. Palsdottir, H., Lojero, C. G., Trumpower, B. L., and Hunte, C. (2003) Structure of the yeast cytochrome bc_1 complex with a hydroxyquinone anion Q_o site inhibitor bound. *J. Biol. Chem.* **278,** 31303–31311
21. Kagawa, Y., and Racker, E. (1971) Partial resolution of the enzymes catalyzing oxidative phosphorylation. XXV. Reconstitution of vesicles catalyzing $^{32}P_i$-adenosine triphosphate exchange. *J. Biol. Chem.* **246,** 5477–5487
22. Yu, C.-A., and Yu, L. (1982) Syntheses of biologically active ubiquinone derivatives. *Biochemistry* **21,** 4096–4101
23. Xiao, K., Liu, X., Yu, C.-A., and Yu, L. (2004) Evidence for electron equilibrium between the two hemes b_L in the dimeric cytochrome bc_1 complex. *Biochemistry* **43,** 1488–1495
24. Mather, M. W., Yu, L., and Yu, C.-A. (1995) The involvement of threonine 160 of cytochrome *b* of *Rhodobacter sphaeroides* cytochrome bc_1 complex in quinone binding and interaction with subunit IV. J. Biol. *Chem.* **270,** 28668–28675
25. Tian, H., Yu, L., Mather, M. W., and Yu, C.-A. (1997) The involvement of serine 175 and alanine 185 of cytochrome *b* of *Rhodobacter sphaeroides* cytochrome bc_1 complex in interaction with iron-sulfur protein. *J. Biol. Chem.* **272,** 23722–23728
26. Berden, J. A., and Slater, E. C. (1970) The reaction of antimycin with a cytochrome *b* preparation active in reconstitution of the respiratory chain. *Biochim. Biophys. Acta* **216,** 237–249
27. Yu, C.-A., Yu, L., and King, T. E. (1972) Preparation and properties of cardiac cytochrome c_1. *J. Biol. Chem.* **247,** 1012–1019
28. Yu, L., Dong, J. H., and Yu, C.-A. (1986) Characterization of purified cytochrome c_1 from *Rhodobacter sphaeroides* R-26. *Biochim. Biophys. Acta* **852,** 203–211
29. Nakano, M. (1990) Determination of superoxide radical and singlet oxygen based on chemiluminescence of luciferin analogs. *Methods Enzymol.* **186,** 585–591
30. Denicola, A., Souza, J. M., Gatti, R. M., Augusto, O., and Radi, R. (1995) Desferrioxamine inhibition of the hydroxyl radical-like reactivity of peroxynitrite: role of the hydroxamic groups. *Free Radic. Biol. Med.* **19,** 11–19
31. Crofts, A. R., Hong, S., Ugulava, N., Barquera, B., Gennis, R., Guergova-Kuras, M., and Berry, E. A. (1999) Pathways for proton release during ubihydroquinone oxidation by the bc_1 complex. *Proc. Natl. Acad. Sci. U.S.A.* **96,** 10021–10026
32. Hunte, C., Koepke, J., Lange, C., Rossmanith, T., and Michel, H. (2000) Structure at 2.3 Å resolution of the cytochrome bc_1 complex from the yeast *Saccharomyces cerevisiae* co-crystallized with an antibody Fv fragment. *Structure* **8,** 669–684
33. Crofts, A. R., Barquera, B., Gennis, R. B., Kuras, R., Guergova-Kuras, M., and Berry, E. A. (1999) Mechanism of ubiquinol oxidation by the bc_1 complex: different domains of the quinol binding pocket and their role in the mechanism and binding of inhibitors. *Biochemistry* **38,** 15807–15826
34. Esposti, M. D., De Vries, S., Crimi, M., Ghelli, A., Patarnello, T., and Meyer, A. (1993) Mitochondrial cytochrome *b*: evolution and structure of the protein. *Biochim. Biophys. Acta* **1143,** 243–271
35. Brasseur, G., Saribaş, A. S., and Daldal, F. (1996) A compilation of mutations located in the cytochrome *b* subunit of the bacterial and mitochondrial bc_1 complex. *Biochim. Biophys. Acta* **1275,** 61–69
36. Covián, R., and Moreno-Sánchez, R. (2001) Role of protonatable groups of bovine heart bc_1 complex in ubiquinol binding and oxidation. *Eur. J. Biochem.* **268,** 5783–5790
37. Leung, K. H., and Hinkle, P. C. (1975) Reconstitution of ion transport and respiratory control in vesicles formed from reduced coenzyme Q-cytochrome *c* reductase and phospholipids. *J. Biol. Chem.* **250,** 8467–8471
38. Güner, S., Robertson, D. E., Yu, L., Qui, Z.-H., Yu, C.-A., and Knaff, D. B. (1991) The *Rhodospirillum rubrum* cytochrome bc_1 complex: redox properties, inhibitor sensitivity and proton pumping. *Biochim. Biophys. Acta* **1058,** 269–279
39. Lorusso, M., Gatti, D., Boffoli, D., Bellomo, E., and Papa, S. (1983) Redox-linked proton translocation in the b-c_1 complex from beef-heart mitochondria reconstituted into phospholipid vesicles. *Eur. J. Biochem.* **137,** 413–420
40. Cocco, T., Lorusso, M., Di Paola, M., Minuto, M., and Papa, S. (1992) Characteristics of energy-linked proton translocation in liposome reconstituted bovine cytochrome bc_1 complex. *Eur. J. Biochem.* **209,** 475–481
41. Gennis, R. B., and Ebrey, T. G. (1999) Proton pump caught in the act. *Science* **286,** 252–253
42. Wikström, M., Verkhovsky, M. I., and Hummer, G. (2003) Water-gated mechanism of proton translocation by cytochrome *c* oxidase. *Biochim. Biophys. Acta* **1604,** 61–65
43. Yang, S., Ma, H. W., Yu, L., and Yu, C.-A. (2008) On the mechanism of quinol oxidation at the Q_P site in the cytochrome bc_1 complex. *J. Biol. Chem.* **283,** 28767–28776
44. Yin, Y., Tso, S. C., Yu, C.-A., and Yu, L. (2009) Effect of subunit IV on superoxide generation by *Rhodobacter sphaeroides* cytochrome bc_1 complex. *Biochim. Biophys. Acta* **1787,** 913–919
45. Yin, Y., Yang, S., Yu, L., and Yu, C.-A. (2010) Reaction mechanism of superoxide generation during ubiquinol oxidation by the cytochrome bc_1 complex. *J. Biol. Chem.* **285,** 17038–17045